Chapter 2
Low-Frequency Electromagnetic Fields and Finite Element Method

Zhiguang Cheng and Norio Takahashi

Abstract Electromagnetic field analysis is the basis for solving the engineering coupled electromagnetic and thermal field problems. Based on the low-frequency Maxwell's equations, some key problems concerning the formulations and numerical implementations of typical 3-D eddy current analysis methods, using different potential sets, such as $\boldsymbol{A}$-V-$\boldsymbol{A}$ (or employing a reduced vector magnetic potential $\boldsymbol{A}_r$ to convert to $\boldsymbol{A}_r$-V-$\boldsymbol{A}_r$) and $\boldsymbol{T}$-Ψ-Ψ, are briefly explained. Furthermore, the numerical solvers based on different potential sets have been developed by the author's group and verified in the Testing Electromagnetic Analysis Methods (TEAM) benchmarking practices. In this chapter, the Galerkin weighted residual method, a key technique in numerical implementation, is elaborated, and the effectiveness of edge element, for example, in effectively reducing computational cost in industrial applications is discussed. Strengthening the theoretical basis of finite element analysis of electromagnetic fields and correctly understanding the significance of the combination of advanced numerical computation with accurate material property modeling will be more helpful in improving the effectiveness of modeling and simulation and further promoting the use of simulation in industrial applications.

Keywords Low-frequency electromagnetic field · Finite element method · Potential set · Nodal element · Edge element · Galerkin weighted residual technique · Formulation and implementation

Z. Cheng (✉)
Institute of Power Transmission and Transformation Technology, Baobian Electric, Baoding, China
e-mail: emlabzcheng@yahoo.com

N. Takahashi (deceased)
Okayama University, Okayama, Japan

© Science Press, Beijing and Springer Nature Singapore Pte Ltd. 2020

Z. Cheng et al. (eds.), *Modeling and Application of Electromagnetic and Thermal Field in Electrical Engineering*, https://doi.org/10.1007/978-981-15-0173-9_2

2.1 Introduction

The related problems involved in engineering electromagnetic and thermal fields are often highly complex. For example, in power transmission and transformation engineering, the critical heating and cooling issues of large power transformers are closely linked to the coupling of electromagnetic field, temperature field and the oil flow field of forced movement. In addition, the influence of temperature, and even stress, must also be considered in electromagnetic property modeling of materials and components, such as nonlinearity, anisotropy and hysteresis of various materials that are inherently complex. However, people do not leave themselves helpless, always trying to solve complex problems, step by step. Moreover, in order to solve the thermal field problem, the power loss, that is the heating source, must be accurately determined first, so electromagnetic field analysis is the basis for solving the problems related to coupled electromagnetic and thermal fields.

There are many classical literatures and monographs on the numerical computation of engineering electromagnetic fields [1–27]. The governing equations of the commonly used eddy current calculations, which can all be derived from Maxwell's equations, and appropriate boundary conditions, gauge and information of field source configuration are introduced to form a definite solution problem. The state variables used may be the field quantities to be solved, such as electric field intensity $\boldsymbol{E}$ and magnetic field intensity $\boldsymbol{H}$, or the vector potential and scalar potential, as well as potential sets thereof.

The finite element method (FEM) is a mature numerical method in industrial applications and is also the main numerical calculation method used in this book. Finite element, as a specialized term, first appeared in 1960 [3]. The usability of finite element was first demonstrated by O. C. Zienkiewicz in the late 1960s and was quickly extended to many application fields in the 1970s.

As far as electrical engineering is concerned, although A. M. Winslow adopted the complete concept of finite element as early as 1967 [6], the finite element method in its present form was applied and popularized by P. P. Silvester and his colleagues two years later [7]. At that time, the element type was mainly nodal element (or node-based element), the edge element (or edge-based element) was first proposed by Fraeijs de Veubeke [4], with its variable defined differently from nodal element, and the constraint of normal continuity of variables along the edge of the element was removed. Raviart and Thomas solved the two-dimensional problem by using the edge element method in 1977, and J. C. Nedelec established a 3-D mixed element model including edge elements and nodal elements by using tetrahedron and hexahedron elements in 1980 [8]. Since the early 1980s, the rapid development of edge element has attracted extensive attention from the international computational electromagnetics community, particularly in theory, numerical implementation and application [26–53]. Moreover, in some applications, the edge element shows its irreplaceable advantages. At the Compumag-1997, in Brazil, a specially arranged discussion meeting on edge element was held. A. Bossavit, Z. Cendes, T. V. Yioultsis, J. P. Webb and G. Mur shared their views in the

discussions, which basically reflected the international computational electromagnetics community's understanding of all aspects of edge element. The theory and practice of edge element have been quite mature, promising a broad prospect of its academic and industrial application.

Edge element and nodal element are two main members of the finite element family and have achieved success in applications. As pointed out by the researchers, they do not replace each other and tend to develop in parallel. It is also shown in research and application that the combination of the two may be more promising, i.e., vector potentials are represented by edge elements, and scalar potentials are represented by nodal elements.

After a very brief review of the FEM as the foundation of electromagnetic and thermal field modeling, this chapter follows the low-frequency Maxwell's equations, introduces several eddy current analysis methods based on various potential sets [24, 25], deduces the basic formulation and numerical implementation and explores the internal relations among various algorithms. The edge element is also briefly discussed and compared with the nodal element, based on the discrete data for the same problem (e.g., total degrees of freedom, number of nonzero entries in the coefficient matrix, etc.). Moreover, based on a typical $\boldsymbol{A}$-V-$\boldsymbol{A}$ method, the main derivation process is demonstrated.

Finally, it should be emphasized that the solid theoretical basis for the finite element analysis of electromagnetic fields, the efficient methods of computation, the accurate modeling of material properties and the tight link between them are most important in improving the effectiveness of modeling and simulation and further promoting the use of simulation in industrial applications.

2.2 Maxwell's Equations

The Maxwell's equations created by J. C. Maxwell (1831–1879) consist of the following four basic equations:

$$\nabla \times \boldsymbol{H} = \boldsymbol{J} + \frac{\partial \boldsymbol{D}}{\partial t} \tag{2.1}$$

$$\nabla \cdot \boldsymbol{B} = \boldsymbol{0} \tag{2.2}$$

$$\nabla \times \boldsymbol{E} = -\frac{\partial \boldsymbol{B}}{\partial t} \tag{2.3}$$

$$\nabla \cdot \boldsymbol{D} = \rho \ (\text{when ignoring the effect of accumulated charge in the conductor } \rho = 0) \tag{2.4}$$

The fifth equation can be obtained from the above equations, that is, taking divergence to the first equation and using the result of the fourth equation, it is derived that

$$\nabla \cdot \boldsymbol{J} = -\frac{\partial \rho}{\partial t} \tag{2.5}$$

which satisfies the following constitutive equations:

$$\boldsymbol{B} = \mu \boldsymbol{H} \tag{2.6}$$

$$\boldsymbol{D} = \varepsilon \boldsymbol{E} \tag{2.7}$$

$$\boldsymbol{J} = \sigma \boldsymbol{E} \tag{2.8}$$

The low-frequency electromagnetic and thermal field are the main research project in this book. $\frac{\partial \boldsymbol{D}}{\partial t}$ in (2.1) can be omitted under the condition of low frequency, considering constitutive relation (2.8), and (2.1) can be rewritten as

$$\nabla \times \boldsymbol{H} = \sigma \boldsymbol{E} \tag{2.9}$$

In general, the phasor form of Eq. (2.1) is

$$\nabla \times \dot{H} = (\sigma + j\varepsilon\omega)\dot{E} \tag{2.10}$$

In the case of low frequency, the second right-hand term of (2.10) can be ignored.

The basic equations related to the complete low-frequency electromagnetic field include the field differential equation and the constitutive equations. Nowadays, with the development of international computational electromagnetics and its application, a series of electromagnetic field analysis methods, based on various "potential sets", have been highly developed and very mature. However, the electromagnetic properties of all the materials involved in the constitutive equations of the basic equations have become the focus of attention.

The material property parameters, σ, ε and μ, relate the basic field quantities $\boldsymbol{J}$, $\boldsymbol{D}$, $\boldsymbol{E}$, $\boldsymbol{B}$ and $\boldsymbol{H}$. Because of the urgent need of scientific research and industrial application, modern material modeling technology endows "σ-ε-μ" with more connotation, such as nonlinearity, time asymmetry, anisotropy and so on. The modeling of electrical, magnetic and thermal properties of electrical engineering materials under standard and non-standard conditions is the basic guarantee for performing effective electromagnetic and thermal analysis. Therefore, both, advanced methods of computation and advanced material models are required.

The material modeling under complex conditions, the implementation and validation of efficient algorithms are interdependent. It is very complicated to model the electromagnetic and other properties of materials under the actual conditions.

The real working conditions of component materials are usually different from the artificially imposed "standard" conditions for testing the properties of materials. In addition, the properties of materials often depend on external conditions such as temperature, frequency and stress, and the real excitation conditions are much more complicated than the imposed "standard" excitation conditions. The natural question is how to properly evaluate the engineering effectiveness of the standard property data and how to correctly handle the calculation results based on the standard property data. The author does not believe that the more complex the problem being studied, the better; however, the measurement and prediction of the "working characteristics" of materials and components under complex conditions is critical to ensuring the effectiveness of modeling and simulation. See Chaps. 7–11 of this book for further details on material modeling.

2.3 Governing Equations for Analysis of Low-Frequency Eddy Current Problems

In the 1980s, the methods of calculating 3-D eddy currents based on various potential sets were fully discussed. The $\boldsymbol{A}$-V-$\boldsymbol{A}$ and $\boldsymbol{T}$-ψ-ψ are two basic eddy current analysis methods, in which $\boldsymbol{A}$ and $\boldsymbol{T}$ are magnetic vector potential and current vector potential, and V and Ψ are electric scalar potential and magnetic scalar potential, respectively [24, 25].

$\boldsymbol{A}$-V-$\boldsymbol{A}$ can easily solve general complex problems, such as nonlinearity, multiply connected regions, multi-subdomains and non-uniform conductivity in conducting regions, which are often encountered in electrical engineering. In the implementation of Galerkin, the interface conditions are naturally met. However, it still has the following disadvantages: It uses vector potentials in the eddy current-free regions, requiring a large amount of memory and a long CPU time. Further research suggests that while $\boldsymbol{A}$-V-$\boldsymbol{A}$ based on nodal element uses magnetic vector potential $\boldsymbol{A}$ in the entire domain, when the Coulomb gauge condition is implemented by inserting penalty function term in the governing equation and there is a great difference in the magnetic permeability between the conducting region and the non-conducting region, the continuity of $\boldsymbol{A}$ and the discontinuity of permeability μ at the interface will force $\nabla \cdot \boldsymbol{A}$ at the interface to jump, which will lead to the decrease of accuracy at the interface. For this reason, O. Biro and others proposed to make the normal component A_n of $\boldsymbol{A}$ discontinuous at the interface to solve this difficulty [27].

$\boldsymbol{T}$-ψ-ψ is another effective method for eddy current analysis. However, despite the many advantages the traditional $\boldsymbol{T}$-ψ-ψ has, such as fewer unknowns and simple numerical implementation, it generally cannot solve the problems of multiply connected regions. There have been some remedies, for example, filling holes in the multiply connected domain with extremely low-conductivity materials, artificially transforming the multiply connected problems into simply connected ones.

Table 2.1 Dual relations of equations of $\boldsymbol{A}$-V-$\boldsymbol{A}$ and $\boldsymbol{T}$-ψ-ψ in conducting regions

Methods	$\boldsymbol{A}$-V-$\boldsymbol{A}$	$\boldsymbol{T}$-Ψ-Ψ
Definition of vector potential	$\boldsymbol{B} = \nabla \times \boldsymbol{A}$	$\boldsymbol{J} = \nabla \times \boldsymbol{T}$
Governing equations in conducting region	$\boldsymbol{H} = \frac{1}{\mu}\nabla \times \boldsymbol{A}$ $\nabla \times \boldsymbol{E} = -\frac{\partial}{\partial t}(\nabla \times \boldsymbol{A})$ $\nabla \times \left(\boldsymbol{E} + \frac{\partial \boldsymbol{A}}{\partial t}\right) = 0$ $\boldsymbol{E} + \frac{\partial \boldsymbol{A}}{\partial t} = -\nabla V'$ $\boldsymbol{E} = -\frac{\partial \boldsymbol{A}}{\partial t} - \nabla V'$	$\boldsymbol{E} = \frac{1}{\sigma}\nabla \times \boldsymbol{T}$ $\nabla \times \boldsymbol{H} = \nabla \times \boldsymbol{T}$ $\nabla \times (\boldsymbol{H} - \boldsymbol{T}) = 0$ $\boldsymbol{H} - \boldsymbol{T} = -\nabla \varphi$ $\boldsymbol{H} = \boldsymbol{T} - \nabla \psi$
	$\nabla \times \frac{1}{\mu}\nabla \times \boldsymbol{A} + \sigma\left(\frac{\partial \boldsymbol{A}}{\partial t} + \nabla V'\right) = 0$	$\nabla \times \frac{1}{\sigma}\nabla \times \boldsymbol{T} + \frac{\partial}{\partial t}(\mu(\boldsymbol{T} - \nabla \psi)) = 0$
	For nodal elements, Coulomb gauge is adopted and penalty function term is introduced $-\nabla \frac{1}{\mu}\nabla \cdot \boldsymbol{A}$ $\nabla \times \frac{1}{\mu}\nabla \times \boldsymbol{A} - \left(\nabla \frac{1}{\mu}(\nabla \cdot \boldsymbol{A})\right) + \sigma\left(\frac{\partial \boldsymbol{A}}{\partial t} + \nabla V'\right) = 0$ it is derived that from $\nabla \cdot \boldsymbol{J} = 0$ $\nabla \cdot \left(-\sigma\left(\frac{\partial \boldsymbol{A}}{\partial t} + \nabla V'\right)\right) = 0$	For nodal elements, Coulomb gauge is adopted and penalty function term is introduced $-\nabla \frac{1}{\sigma}\nabla \cdot \boldsymbol{T}$ $\nabla \times \frac{1}{\sigma}\nabla \times \boldsymbol{T} - \left(\nabla \frac{1}{\sigma}(\nabla \cdot \boldsymbol{T})\right) + \frac{\partial}{\partial t}(\mu(\boldsymbol{T} - \nabla \psi)) = 0$ it is derived that from $\nabla \cdot \boldsymbol{B} = 0$ $\nabla \cdot (\mu(\boldsymbol{T} - \nabla \psi)) = 0$

There are also handling means such as so-called cutting surface or auxiliary coils arranged around the holes (see Sect. 4.4 of Chap. 4 of this book) to solve the problem of "multiply connected" in the traditional $\boldsymbol{T}$-Ψ-Ψ. The systematic evaluation, comparison and discussion of various eddy current analysis methods and element types have been found in many references, which are of great significance for in-depth understanding of the advantages and disadvantages of various methods and correct selection of analysis methods.

The derivation of governing equations for $\boldsymbol{A}$-V-A and $\boldsymbol{T}$-Ψ-Ψ is of typical significance, and the derivation of governing equations for the corresponding conducting regions is shown in Table 2.1.

The dual relationship between $\boldsymbol{A}$-V-$\boldsymbol{A}$ and $\boldsymbol{T}$-ψ-ψ can be clearly seen from Table 2.1, and even the derivation steps are completely coherent. The derivation process of $\boldsymbol{A}$-V-$\boldsymbol{A}$ based on nodal element using Galerkin weighted residual technique is shown in Appendix.

It should be pointed out that in order to simplify the finite element pre-processing of complex excitation sources and improve the calculation accuracy, relevant reduced potentials are often used in the development of eddy current analysis software based on $\boldsymbol{T}$-Ψ-Ψ and $\boldsymbol{A}$-V-$\boldsymbol{A}$ potential sets. For instance, in $\boldsymbol{A}$-V-$\boldsymbol{A}$,

a reduced magnetic vector potential, $\boldsymbol{A}_r$, is adopted, i.e., converting it to $\boldsymbol{A}_r$-V-$\boldsymbol{A}_r$; in the implementation of $\boldsymbol{T}$-Ψ-Ψ, a reduced magnetic scalar potential φ is adopted, i.e., $\boldsymbol{T}$-φ-φ [24, 25].

2.4 $\boldsymbol{A}_r$-V-$\boldsymbol{A}_r$-Based Method

$\boldsymbol{A}_r$-V-$\boldsymbol{A}_r$ [25] can simplify the 3-D grid meshing of complex excitation source structure and eliminate the error caused by inaccurate excitation conditions due to the difference between the grid and the source structure entity, reducing the amount of grid and the computing cost. The numerical solver based on $\boldsymbol{A}_r$-V-$\boldsymbol{A}_r$ potential set has been developed by the author and applied to the calculation of loss, magnetic flux density at designated position and interlinkage flux in the conducting component of the Testing Electromagnetic Analysis Methods (TEAM) Problem 21 benchmark models (the updated version of Problem 21 Family is posted at www.compumag.org/team), which has been validated through repeated comparisons of calculation and measurement results. Refer to the results of Chap. 12 of this book.

There is no substantial difference in the numerical implementation between $\boldsymbol{A}_r$-V-$\boldsymbol{A}_r$ and $\boldsymbol{A}$-V-$\boldsymbol{A}$. Where the total magnetic vector potential $\boldsymbol{A}$ is divided into two parts, i.e., the total magnetic vector potential $\boldsymbol{A}$ at any point in the field is synthesized by the contribution $\boldsymbol{A}_s$ of the excitation source and all contributions $\boldsymbol{A}_r$ other than the contribution of source

$$\boldsymbol{A} = \boldsymbol{A}_r + \boldsymbol{A}_s \tag{2.11}$$

where $\boldsymbol{A}_s$ is defined as being generated only by the excitation source in free space, which can be derived by Biot Savart Law, while $\boldsymbol{A}_r$ is a contribution other than the contribution of excitation source, which is an unknown variable to be solved and is called the reduced magnetic vector potential. $\boldsymbol{A}_s$ can be derived from (2.12)

$$\boldsymbol{A}_s = \frac{\mu_0}{4\pi}\int \frac{i d\boldsymbol{l}}{r} \tag{2.12}$$

Based on the magnetic field intensity $\boldsymbol{H}_s$ generated by the excitation source, it can be calculated by Eq. (2.13) that is

$$\boldsymbol{H}_s = \frac{1}{4\pi}\int \frac{i d\boldsymbol{l} \times \boldsymbol{r}}{r^3} \tag{2.13}$$

Problems needing attention in the numerical implementation and application of $\boldsymbol{A}_r$-V-$\boldsymbol{A}_r$ are as follows:

(1) When establishing the tangential continuity condition $\boldsymbol{H} \times \boldsymbol{n}$ of magnetic field intensity based on nodal elements, attention should be paid to the relationship

of $\boldsymbol{A} = \boldsymbol{A_r} + \boldsymbol{A_s}$, that is, the total magnetic vector potential is composed of two components;

(2) Similarly, based on the far field boundary (or magnetic symmetry plane) of nodal element, $\boldsymbol{B_n} = 0$ is expressed as

$$(\boldsymbol{A_r} + \boldsymbol{A_s}) \times \boldsymbol{n} = 0 \tag{2.14}$$

Far field boundary $\boldsymbol{H_t} = 0$ is expressed as

$$(\boldsymbol{A_r} + \boldsymbol{A_s}) \cdot \boldsymbol{n} = 0 \tag{2.15}$$

At infinitely far points

$$\boldsymbol{A_r} + \boldsymbol{A_s} = 0 \tag{2.16}$$

(3) The application practice shows that it is very important to calculate $\boldsymbol{A_s}$ and $\boldsymbol{H_s}$ correctly. In order to confirm the accuracy of the calculation, $\boldsymbol{A_s}$ and $\boldsymbol{H_s}$ can be calculated according to Eqs. (2.12) and (2.13), respectively, and $\boldsymbol{B_s}$ can be calculated based on $\boldsymbol{A_s}$ and $\boldsymbol{H_s}$, respectively, i.e.,

$$\boldsymbol{B_{s1}} = \mu_0 \boldsymbol{H_s} \tag{2.17}$$

$$\boldsymbol{B_{s2}} = \nabla \times \boldsymbol{A_s} \tag{2.18}$$

Then compare the results of $\boldsymbol{B_s}$ obtained according to Eqs. (2.17) and (2.18).

2.5 Scalar and Vector Galerkin Weight Function

Galerkin weighted residual method is one of the weighted residual techniques, and it is one of the key techniques in the numerical implementation of 3-D eddy current analysis method based on various potential sets (combination of vector potentials and scalar potentials).

After the Galerkin method was put forward in 1915, the weighted residual technique has gone through more than 40 years of development. The Galerkin method, integral method, subdomain method, least square method, moment method and other processing techniques were successively put forward and were collectively summarized as the weighted residual method by S. H. Crandall in 1956 [15].

As well known, the finite element method is an approximation of the actual continuous physical field. Taking the nodal element as an example, let the number of nodes be N_n, and the state variable φ can be expressed by the variable value φ_i and the shape function N_i (or experimental function) of the node as

$$\phi = \sum_{i=1}^{N_n} N_i \phi_i \tag{2.19}$$

As an approximate solution, it is impossible to accurately satisfy the governing equation, and the resulting error is called the residual $R(\varphi)$. It is necessary to find a weight function, for example, W_i, to force the inner product of the residual and the weight function to be zero, i.e.,

$$\langle R(\varphi), W_i \rangle = 0, \quad i = 1, 2, \ldots, N_n \tag{2.20}$$

This means that the residual is equal to 0 in the sense of weighted average. When the weight function W_i is consistent with the shape function N_i used, it is known as the Galerkin weighted residual method.

In the references on 3-D eddy current analysis, the weighted residual technique is widely used in numerical implementations. Galerkin method is used to deal with the vector eddy current equation, sometimes the scalar weight function W_i is used, and more often the vector weight function $\boldsymbol{N_i}$ is used. The formula derivation of nodal element based on scalar weight function and vector weight function shows that they present only differences in forms because the results obtained are completely consistent. The vector weight function makes the expression simple, and the scalar weight function has the advantages of clear hierarchy and easy deduction.

For the detailed deduction of Galerkin process based on edge element, it is suggested to refer to the related references [17]. Section 2.7 of this chapter only gives a comparison between the nodal element and the edge element with respect to Galerkin's residual.

2.6 Discussion on Edge Elements

A. Bossavit has made the following penetrating elaboration: In short, the finite element shall not be viewed in isolation; the finite element is expected to be used to approximately all the potentials and fields involved in Maxwell's equations, such as edge elements, nodal elements, facet elements and volume elements, which can be regarded as a consistent expression system, called the family of cell elements.

The edge element is closely related to the corresponding nodal elements. The difference between edge element and nodal element in discretization is a shape function. It can be said that if the analysis software based on edge element (nodal element) has been developed separately, it is not difficult to develop the software of new nodal element (edge element).

The application of edge element in electromagnetic field was pioneered by the French research group represented by A. Bossavit. Since the 1980s, edge element has been widely used in the field of electromagnetic fields. When it comes to the starting point of the development of edge elements, it is necessary to trace back the

history of the development of $\boldsymbol{H}$-ψ. In $\boldsymbol{H}$-ψ, the magnetic field intensity $\boldsymbol{H}$ is directly used as the state variable in the eddy current region, instead of the traditional use of a certain potential, e.g., magnetic vector potential $\boldsymbol{A}$, and magnetic scalar potential ψ is used in the non-eddy current region. Since the magnetic field intensity $\boldsymbol{H}$ is used as the state variable, the required field quantity can be directly obtained, and it also has the advantages of easy handling of nonlinear problems (the permeability reflecting the nonlinearity of the material is not embedded in the differential operator). If the magnetic vector potential $\boldsymbol{A}$ is used as the state variable, the problem is that the coupling of $\boldsymbol{A}$-ψ generates a coefficient matrix that is either asymmetric or indefinite. However, if $\boldsymbol{H}$-ψ of nodal element is adopted, it will be difficult to deal with the tangential continuity of the coupling between eddy current region ($\boldsymbol{H}$) and non-eddy current region (ψ). It is in such a background that the edge element enters the field of computational electromagnetics.

The appearance of the edge element has attracted great attention in the field of computational electromagnetics and a great deal of research in theory, numerical implementation and gauge condition. Based on typical examples and very specific cases, a comprehensive and in-depth comparison is made between the edge element and the nodal element, and the advantages and disadvantages of edge element are discussed [28, 48]. It should be noted that Z. Ren and K. Shao et al. proposed hybrid FEM–BIM formulation and edge–nodal coupled model in 1990s, as well as related application [37, 51–53].

This chapter has made a systematic comparison of the two kinds of finite elements in another monograph [54] and pointed out that the role of nodal elements and edge elements should be correctly evaluated. Although the edge element has advantages over the nodal element in dealing with the problem of uniform or non-uniform regions (especially the latter), however, it is exaggerated to think that the edge element can surpass the nodal element in solving any difficulties encountered in electromagnetic field analysis, and that the accurate solution can be obtained only by using edge elements. It depends on what problems are being solved and what state variables are being used. We should consider the advantages of the edge element, as well as its disadvantages in some occasions or limitations in application. As G. Mur said, the point here is that when the right solution is derived, and it should be attributed to the applied finite element method, not to the edge element [28].

In edge element, when the magnetic vector potential $\boldsymbol{A}$ is a state variable, the normal continuity of magnetic flux density and current density ($\boldsymbol{B}$ and $\boldsymbol{J}$) is strictly guaranteed because the tangential component of $\boldsymbol{A}$ at the element interface is continuous, while the tangential continuity of magnetic field intensity and electric field intensity ($\boldsymbol{H}$ and $\boldsymbol{E}$) can only be weakly satisfied. When the magnetic field intensity $\boldsymbol{H}$ is a state variable, the continuity condition of the magnetic field intensity is strictly guaranteed because the tangential component of $\boldsymbol{H}$ at the element interface is continuous, while the normal continuity of the magnetic flux density ($\boldsymbol{B}$) also can only be weakly satisfied.

Besides, further research shows that if the continuity condition of the excitation current density cannot be strictly guaranteed, the convergence of the solution cannot be achieved through general ICCG methods when the edge element is used [30, 44].

It is hoped that these discussions will contribute to a better understanding of edge elements.

2.7 Comparison of Basic Equations and Galerkin Residuals of Nodal Elements and Edge Elements

When solving a problem related to low-frequency electromagnetic field, the basic equations in the conducting region may be different due to the different types of elements used. For example, the $\boldsymbol{A}$-V based on nodal elements uses magnetic vector potential $\boldsymbol{A}$ and electric scalar potential V in the conducting region, wherein each node contains four unknowns which requires four equations, and the basic equation consists of a vector equation and a scalar equation. However, based on the basic equation of the edge element, as shown in Table 2.2, when no electric scalar potential V is introduced, only the magnetic vector potential $\boldsymbol{A}$ is used. Therefore, there is only one vector equation and no scalar equation corresponding to the nodal element.

In addition, the gradient term of the electric scalar potential V in the expression G_e of Galerkin residual of the corresponding edge element will not appear, which is different from the expression G_n of Galerkin residual of the nodal element. Naturally, for the edge element, there is no expression G_{ns} of Galerkin residual corresponding to the nodal element, as shown in Table 2.2.

It should be pointed out that (1) For nodal elements, using scalar weight function N_i and vector weight function $\boldsymbol{N_i}$ will get the same results in Galerkin weighted residual processing [54]; (2) Although the weight functions $\boldsymbol{N_i}$ in the nodal element residual G_n (when vector weight function is used) and the edge element residual G_e are written using the same vector symbol, as shown in Table 2.2, their contents are completely different. Appendix shows the formulation of $\boldsymbol{A}$-V-$\boldsymbol{A}$ and Galerkin weighted residual processing.

2.8 Comparison of Nonzero Entries and Total Unknowns in Coefficient Matrix

The total unknowns and the number of nonzero entries in the coefficient matrix vary with the calculation method, the type of finite element (e.g., nodal element or edge element) and the ratio α of the number of elements in the conducting region to the number of elements in the entire solved domain, which directly affects the computer memory requirement and CPU time.

Table 2.2 Comparison of basic equations and Galerkin residuals of nodal elements and edge elements (***A*-*V*-*A***)

Element type	Basic equation (in conducting region)	Galerkin residual
Nodal element	$\nabla \times (\nu \nabla \times \boldsymbol{A}) = \boldsymbol{J}_0 - \sigma\left(\frac{\partial \boldsymbol{A}}{\partial t} + \nabla V\right)$	Using vector weight function $\boldsymbol{N_i}$: $G_n = \int_V \nabla \times \boldsymbol{N}_i \cdot (\nu \nabla \times \boldsymbol{A}) \mathrm{d}v - \int_{vc} \boldsymbol{N}_i \cdot \boldsymbol{J}_0 \mathrm{d}v + \int_{ve} \left[\boldsymbol{N}_i \cdot \left(\frac{\partial \boldsymbol{A}}{\partial t} + \nabla V\right)\right] \mathrm{d}v - \int_s \boldsymbol{N}_i \cdot [(\nu \nabla \times \boldsymbol{A}) \times \boldsymbol{n}] \mathrm{d}s$ Using scalar weight function N_i: $G_n = -\int_v \nabla N_i \times (\nu \nabla \times \boldsymbol{A}) \mathrm{d}v - \int_{vc} N_i \boldsymbol{J}_0 \mathrm{d}v + \int_{ve} N_i \left[\sigma\left(\frac{\partial \boldsymbol{A}}{\partial t} + \nabla V\right)\right] \mathrm{d}v + \int_s N_i \boldsymbol{n} \times (\nu \nabla \times \boldsymbol{A}) \mathrm{d}s$
	$\nabla \cdot \left[-\sigma\left(\frac{\partial \boldsymbol{A}}{\partial t} + \nabla V\right)\right] = 0$	$G_{ns} = \int_{ve} \nabla N_i \cdot \left[\sigma\left(\frac{\partial \boldsymbol{A}}{\partial t} + \nabla V\right)\right] \mathrm{d}v + \int_{se} N_i \left[-\sigma\left(\frac{\partial \boldsymbol{A}}{\partial t} + \nabla V\right)\right] \cdot \boldsymbol{n} \mathrm{d}s$
Edge element	$\nabla \times (\nu \nabla \times \boldsymbol{A}) = \boldsymbol{J}_0 - \sigma \frac{\partial \boldsymbol{A}}{\partial t}$	$G_e = \int_V \nabla \times \boldsymbol{N}_i \cdot (\nu \nabla \times \boldsymbol{A}) \mathrm{d}v - \int_{\mathrm{vc}} \boldsymbol{N}_i \cdot \boldsymbol{J}_0 \mathrm{d}v + \int_{ve} \boldsymbol{N}_i \cdot \sigma \frac{\partial \boldsymbol{A}}{\partial t} \mathrm{d}v - \int_s \boldsymbol{N}_i \cdot [(\nu \nabla \times \boldsymbol{A}) \times \boldsymbol{n}] \mathrm{d}s$

This section proposes a method to estimate the total number of both the unknowns and the nonzero entries in the coefficient matrix for the same problem but using either edge elements or nodal elements and examines the effectiveness of edge elements by comparing the estimated results [49].

Only the $\boldsymbol{A}$-V-$\boldsymbol{A}$ (also known as $\boldsymbol{A}$-ϕ) based on the brick element is taken as an example in the following analysis and comparison. It is assumed that the number of elements in the solved domain is so large that the reduction of unknowns due to the processing of boundary conditions can be ignored, and the use of gauge condition is not considered.

2.8.1 Unknowns and Number of Nonzero Entries in Matrix

2.8.1.1 Nodal Element

For a regular hexahedron (brick), the node number of an element is 8, and a node belongs to 8 elements, as shown in Fig. 2.1a. When the number of elements is very large, the average node number per element is 1 (=8/8). Therefore, the total number of elements ne and the total number of nodes nt have the following relationship:

$$nt = ne \tag{2.21}$$

In the nodal element-based $\boldsymbol{A}$-V-$\boldsymbol{A}$, each node in the conducting region Rj has four unknowns, i.e., the electric scalar potential V and three components of magnetic vector potential $\boldsymbol{A}$, while in the air region Ro, each node has three unknowns, namely three components of $\boldsymbol{A}$. Therefore, the total unknowns nu can be expressed as

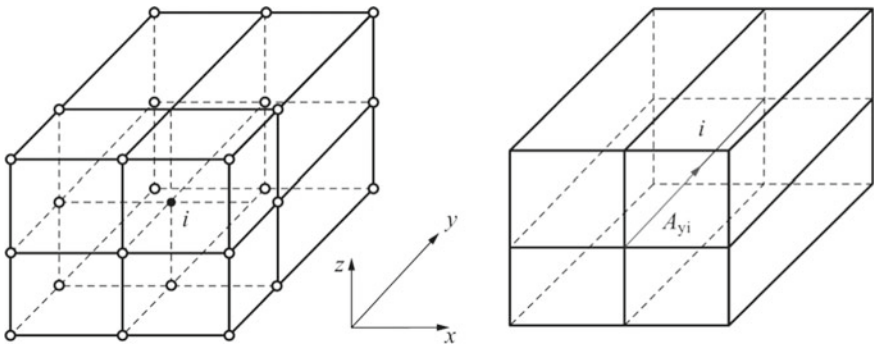

(a) Nodal element (b) Edge element

Fig. 2.1 Nodal element and edge element

$$\begin{aligned} nu(\text{nodal}, \boldsymbol{A}-V-\boldsymbol{A}) &= 4\alpha nt + 3\,(1-\alpha)nt \\ &= (\alpha+3)ne \end{aligned} \tag{2.22}$$

where α represents the percentage of the number of elements in the conducting region Rj to the total number of elements in the solution region (Rj + Ro). It is noted that the relation of $nt = ne$ under the condition that a large number of brick elements are introduced in Eq. (2.22). Since the node number associated with a node i is 27, as shown in Fig. 2.1a, the unknowns associated with node i in the conducting region are 27×4, while the unknowns associated with a node i in the air region are 27×3. In the case of nodal element, the number nz (nodal, $\boldsymbol{A}$-V-$\boldsymbol{A}$) of nonzero entries in the coefficient matrix can be expressed as

$$\begin{aligned} nz(\text{nodal}, \boldsymbol{A}-V-\boldsymbol{A}) &= 4\alpha nt \times 27 \times 4 + 3(1-\alpha)nt \times 27 \times 3 \\ &= 27(7\alpha+9)ne \end{aligned} \tag{2.23}$$

2.8.1.2 Edge Element

The number of edges in a brick element is 12, and the number of elements sharing one edge is 4, as shown in Fig. 2.1b. When the number of elements is very large, the average number of edges per element is 3 (=12/4). Therefore, the total number of elements ne and the total number of edges nh have the following relationship:

$$nh = 3ne \tag{2.24}$$

In $\boldsymbol{A}$-V-$\boldsymbol{A}$ using edge element, V can be set to zero [29]. Only one component of the magnetic vector potential $\boldsymbol{A}$ is defined on one edge. For example, only the y component Ayi is defined on the i-th edge, as shown in Fig. 2.1b. Therefore, the total unknowns nu (edge, $\boldsymbol{A}$-V-$\boldsymbol{A}$) can be expressed as

$$\begin{aligned} nu(\text{edge}, \boldsymbol{A}-V-\boldsymbol{A}) &= nh + \alpha nt = 3ne + \alpha nt \\ &= (\alpha+3)ne \end{aligned} \tag{2.25}$$

Here, the total number of edges associated with the i-th edge is 33, while the number of nodes associated with this edge is 18, as shown in Fig. 2.1b. Therefore, the total number of nonzero entries nz (edge, $\boldsymbol{A}$-V-$\boldsymbol{A}$) is

$$nz(\text{edge}, \boldsymbol{A}-V-\boldsymbol{A}) = 3ne \times 33 + \alpha nt \times 18 = (99+18\alpha)ne \tag{2.26}$$

where the meanings of ne, α and nt are the same as before.

According to the same approach, the number of unknowns in $\boldsymbol{T}$-Ψ-Ψ (also known as $\boldsymbol{T}$-Ω) and the number of nonzero entries in the matrix can be estimated.

2.8.2 Comparison of Nonzero Entries and Total Unknowns in Matrix

Equations (2.22) and (2.25) show that the total unknowns of the regular-hexahedron nodal element and the regular-hexahedron edge element are equal under the condition that the influence of the treatment of boundary conditions (possibly leading to a decrease in the unknowns) is not taken into account.

However, Eqs. (2.23) and (2.26) indicate that the numbers of nonzero entries in the element matrices are far from being equal.

The estimation method proposed in this section is verified by a 3-D eddy current verification model [50] proposed by IEEJ (IEE of Japan). IEEJ eddy current model is a section of square core surrounded and excited by a coil with a race track-shaped cross section. The core and the exciting coil are equal in height, and a square aluminum plate is symmetrically placed above and below the core and the exciting coil; the aluminum plate can be either with hole or without hole. See Fig. 2.2 for the structure and size, material property parameters and excitation ampere turns of the model of the aluminum plate with hole.

The model is calculated by $\boldsymbol{A}$-V-$\boldsymbol{A}$ and $\boldsymbol{T}$-Ψ-Ψ and two types of elements (nodal element and edge element), respectively. See Table 2.3 for numerical computation data and CPU time.

The comparison of computation data of the same problem, two types of elements and two analysis methods shown in Table 2.3 can be summarized as follows:

(1) The total unknowns of $\boldsymbol{A}$-V-$\boldsymbol{A}$ and $\boldsymbol{T}$-Ψ-Ψ are nearly equal, the number of unknowns of the nodal elements is slightly larger than that of the edge elements, and the increment is about 2–5%.
(2) The difference in the number of nonzero entries in the coefficient matrix is larger. The number of nonzero entries in the matrix of nodal elements in $\boldsymbol{A}$-V-$\boldsymbol{A}$ is about 2.7 times that of edge elements, while the number of nonzero entries in the matrix of nodal elements in $\boldsymbol{T}$-Ψ-Ψ is about 1.5 times that of edge elements.

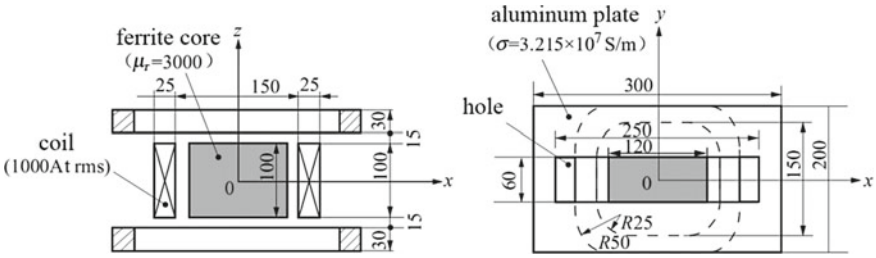

Fig. 2.2 Verification model (IEEJ)

Table 2.3 Numerical computation data and CPU time

Discrete and calculating data	Without hole				With hole			
	A*-*V*-*A		***T*-Ψ-Ψ**		***A*-*V*-*A***		***T*-Ψ-Ψ**	
	Nodal element	Edge element	Nodal element	Edge element	Nodal element	Edge element	Nodal element	Edge element
Total number of elements	14,400							
Total number of nodes	16,275							
Total number of unknowns	43,417	41,060	22,844	22,412	42,885	41,060	22,844	22,412
Number of matrix nonzero entries	1,781,644	653,718	632,859	423,056	1,734,684	653,718	632,859	423,056
Memory Requirements (MB)	72.2	28.4	30.7	19.4	70.5	28.4	30.7	19.4
Number of ICCG iterations	1306	513	172	192	1264	582	1141	327
CPU time (s)	6242	947	533	290	5870	1069	2001	442

Notes

(1) Computer used: NEC supercomputer SX-1E (285MFLOPS)

(2) ICCG convergence criterion: 10^{-7}

(3) The ratio of the number of elements in the conducting region to the total number of elements in solved region α

$\alpha = 0.14$ (with hole); $\alpha = 0.18$ (without hole)

(3) The difference in the memory requirement of the computer is larger. The memory requirement of the nodal element in $\boldsymbol{A}$-V-$\boldsymbol{A}$ is about 2.5 times that of the edge elements, while the memory requirement ratio in $\boldsymbol{T}$-Ψ-Ψ is more than 1.5 times.
(4) The CPU time of the nodal element in $\boldsymbol{A}$-V-$\boldsymbol{A}$ is 5.5–6.5 times that of the edge element, while the ratio of the CPU times in $\boldsymbol{T}$-Ψ-Ψ is 1.8–4.5 times or above.

Memory requirements, depending on the total unknowns of the problem to be solved and the number of nonzero entries in the finite element coefficient matrix, may become a "bottleneck" when using simulation in industrial applications. The above discussion is based on brick element. It is easy to understand that the number of nonzero entries in the coefficient matrix is related to the number of elements associated with nodes and edges. One of the hexahedron nodal elements is associated with eight brick elements, while one edge of the hexahedron edge element is associated with only four brick elements. Therefore, the "density" of nonzero entries in the coefficient matrix of edge elements is smaller than that of nodal elements.

2.9 Concluding Remarks

In this chapter, based on the fundamental equations of low-frequency electromagnetic fields, the dual relation between $\boldsymbol{A}$-V-$\boldsymbol{A}$ and $\boldsymbol{T}$-ψ-ψ, as the basic eddy current analysis methods, is discussed, and the numerical implementation process of the Galerkin weighted residual method is deduced. The two most important members of the finite element family, nodal element and edge element are compared in multi-aspects, revealing their differences and internal relations. All the deductions of the formulation and the numerical implementation based on typical potential sets, in an easy to understand way, and the related discussions on the development and progress of the finite element method are of help for finite element investigation and application.

Taking the brick element used in large-scale finite element analysis as an example, when the edge element and the nodal element have the same mesh, the number of unknowns is similar between the two; however, the number of nonzero entries in the coefficient matrix of the edge element is significantly smaller than that of the nodal element. Therefore, the CPU time required in general is less, indicating that the edge element can effectively reduce the computing cost.

Furthermore, the combination of advanced numerical computation and accurate material property modeling is emphasized in order to improve the effectiveness of modeling and simulation and to promote the large-scale industrial application.

Acknowledgements This work was supported in part by the Natural Science Foundation of China (no. 59277296 and no. 59924035). In particular, the author appreciates the support of the leaders concerned and thanks all the colleagues for joint development of 3-D eddy current field solvers for years.

Appendix: Formulation of *A-V-A* and Galerkin Weighted Residual Processing

The Galerkin's weighted residual processing is demonstrated based on the potential set of ***A-V-A*** using nodal element. Although the model shown in Fig. 2.3 looks simple, but it does not lose generality. For the more general case, there is no substantial difference or difficulty in the derivation process here. This is helpful for knowing basic derivation process.

Basic Model of *A-V-A*

In the ***A-V-A*** model, ***A*** (magnetic vector potential) and V (electric scalar potential) are used in the conductor—eddy current region, and only the magnetic vector potential ***A*** is used outside the conducting region.

Where σ and μ are the conductivity and permeability of the conducting material, respectively, and the magnetic anisotropy and nonlinearity needed to be considered. In the non-conducting region, the conductivity σ is zero, and the relative permeability μ_r is equal to 1.

The symbols in Fig. 2.3 are given the following meanings:

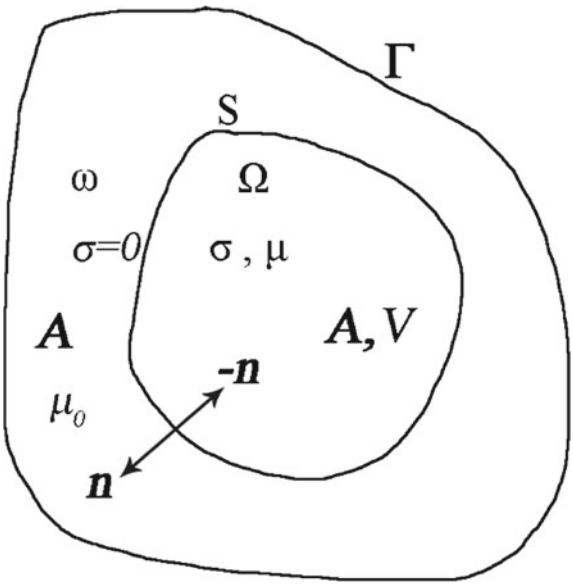

Fig. 2.3 ***A-V-A*** model

ω non-eddy current region, Ω: eddy current region
S interface between eddy current region and non-eddy current region
$\boldsymbol{n}$ exterior normal unit vector of conductor surface in eddy current region
$\boldsymbol{n}'$ internal normal unit vector of conductor surface in eddy current region, where

$$\boldsymbol{n}' = -\boldsymbol{n} \tag{2.27}$$

Γ: The outer boundary of the whole solution domain, including generally the following two types:

$$\Gamma_h: \boldsymbol{H} \times \boldsymbol{n} = 0 \tag{2.28}$$

$$\Gamma_b: \boldsymbol{B} \cdot \boldsymbol{n} = 0 \tag{2.29}$$

$\boldsymbol{A}$ magnetic vector potential (Wb/m)
V integral quantity of electric scalar potential V' to time (Vs)

$$V = \int V' \mathrm{d}t \tag{2.30}$$

μ permeability of conductor (H/m)
σ Conductor conductivity (S/m), where the material is set to electric linear and σ is constant

Considering that the permeability of the material in the eddy current region of conductor is treated as anisotropic in any direction, its general tensor form is

$$\bar{\mu} = \begin{bmatrix} \mu_{xx} & \mu_{xy} & \mu_{xz} \\ \mu_{yx} & \mu_{yy} & \mu_{yz} \\ \mu_{zx} & \mu_{zy} & \mu_{zz} \end{bmatrix} \tag{2.31}$$

The reluctivity of the material should, therefore, be expressed as follows:

$$\bar{\nu} = [\bar{\mu}]^{-1}$$

It should be pointed out that only for the sake of simplicity of deduction, the anisotropic permeability in the following formula is simply written as μ, and the anisotropic reluctivity is simply written as $\frac{1}{\mu}$.

Definition: $\boldsymbol{B} = \nabla \times \boldsymbol{A}$.

Governing Equation of *A-V-A*

The governing equations of ***A-V-A*** are as follows:

Eddy Current Region

$$\nabla \times \frac{1}{\mu} \nabla \times \boldsymbol{A} - [\nabla \frac{1}{\mu_c} \nabla \cdot \boldsymbol{A}] + \sigma \left(\frac{\partial \boldsymbol{A}}{\partial t} + \nabla \frac{\partial V}{\partial t} \right) = 0 \tag{2.32}$$

In square brackets of Eq. (2.32) is a penalty function term to enforce the zero divergence condition, the same below, where μ_c needs to be isotropic to ensure the symmetry of the coefficient matrix. μ_c can be determined by the permeability of neighboring elements and updated during iteration.

$$\nabla \cdot \sigma \left(-\frac{\partial \boldsymbol{A}}{\partial t} - \nabla \frac{\partial V}{\partial t} \right) = 0 \tag{2.33}$$

Non-Eddy Current Region

$$\nabla \times \frac{1}{\mu_0} \nabla \times \boldsymbol{A} - \nabla \frac{1}{\mu_0} \nabla \cdot \boldsymbol{A} = 0 \tag{2.34}$$

where μ_0: permeability in air.

Galerkin Weighted Residual Processing

Galerkin Residuals

The Galerkin weighted residual technique is applied to (2.32)–(2.34), and the continuity condition of the boundary field quantity ($\boldsymbol{B}$, $\boldsymbol{H}$) is considered.

$$(\boldsymbol{B}_1 - \boldsymbol{B}_2) \cdot \boldsymbol{n} = 0 \tag{2.35}$$

$$(\boldsymbol{H}_1 - \boldsymbol{H}_2) \times \boldsymbol{n} = 0 \tag{2.36}$$

The discretization equation is derived. The subscripts 1 and 2 indicate both sides of the interface.

The Galerkin residuals corresponding to (2.32) and (2.33), using scalar weight function, are, respectively, as follows:

$$\boldsymbol{R_1} = \int_{\Omega} N_i \left(\nabla \times \frac{1}{\mu} \nabla \times \boldsymbol{A} - \nabla \frac{1}{\mu_c} \nabla \cdot \boldsymbol{A} + \sigma \left(\frac{\partial \boldsymbol{A}}{\partial t} + \nabla \frac{\partial V}{\partial t} \right) \right) \mathrm{d}v \tag{2.37}$$

$$R_0 = \int_{\Omega} N_i \nabla \cdot \sigma \left(- \frac{\partial \boldsymbol{A}}{\partial t} - \nabla \frac{\partial V}{\partial t} \right) \mathrm{d}v \tag{2.38}$$

where N_i is a scalar weight function. For ease of derivation, $\boldsymbol{R}_1$ is rewritten separately as three terms

$$R_{11} = \int_{\Omega} N_i \nabla \times \frac{1}{\mu} \nabla \times \boldsymbol{A} \, \mathrm{d}v \tag{2.39}$$

$$R_{12} = - \int_{\Omega} N_i \nabla \frac{1}{\mu_c} \nabla \cdot \boldsymbol{A} \, \mathrm{d}v \tag{2.40}$$

$$R_{13} = \int_{\Omega} N_i \sigma \left(\frac{\partial \boldsymbol{A}}{\partial t} + \nabla \frac{\partial V}{\partial t} \right) \mathrm{d}v \tag{2.41}$$

Residuals Processing

Eddy Current Region

For (2.39), the vector formulation is

$$\nabla \times \left(N_i \frac{1}{\mu} \nabla \times \boldsymbol{A} \right) = \nabla N_i \times \frac{1}{\mu} \nabla \times \boldsymbol{A} + N_i \nabla \times \frac{1}{\mu} \nabla \times \boldsymbol{A} \tag{2.42}$$

(2.42) is sorted out to:

$$N_i \nabla \times \frac{1}{\mu} \nabla \times \boldsymbol{A} = \nabla \times \left(N_i \frac{1}{\mu} \nabla \times \boldsymbol{A} \right) - \nabla N_i \times \frac{1}{\mu} \nabla \times \boldsymbol{A} \tag{2.43}$$

Substituting (2.43) into (2.39)

$$R_{11} = \int_{\Omega} \nabla \times \left(N_i \frac{1}{\mu} \nabla \times \boldsymbol{A} \right) \mathrm{d}v - \int_{\Omega} \nabla N_i \times \frac{1}{\mu} \nabla \times \boldsymbol{A} \, \mathrm{d}v \tag{2.44}$$

The vector formulation is

$$\int_{\Omega} \nabla \times \boldsymbol{a}\, \mathrm{d}v = \oint_{s} \boldsymbol{n} \times \boldsymbol{a}\, \mathrm{d}s$$

(2.44) can be rewritten as follows:

$$R_{11} = -\oint_{s} N_i \boldsymbol{n} \times \frac{1}{\mu} \nabla \times \boldsymbol{A}\, \mathrm{d}s - \int_{\Omega} \nabla N_i \times \frac{1}{\mu} \nabla \times \boldsymbol{A}\, \mathrm{d}v \tag{2.45}$$

Apparently, $\boldsymbol{n} \times \frac{1}{\mu} \nabla \times \boldsymbol{A} = \boldsymbol{n} \times \boldsymbol{H}$ is the tangential component of the magnetic field intensity at the interface. According to the continuity condition of the tangential component of the magnetic field intensity at the interface, the surface integral in (2.45) will be canceled from each other with the corresponding surface integral in the non-eddy current region ω derived from (2.34), and then (2.45) contains only the volume integral term, i.e.,

$$R_{11} = -\int_{\Omega} \nabla N_i \times \frac{1}{\mu} \nabla \times \boldsymbol{A}\, \mathrm{d}v \tag{2.46}$$

The vector formulation is

$$\nabla N_i = \frac{\partial N_i}{\partial x}\boldsymbol{i} + \frac{\partial N_i}{\partial y}\boldsymbol{j} + \frac{\partial N_i}{\partial z}\boldsymbol{k} \tag{2.47}$$

$$\frac{1}{\mu} \nabla \times \boldsymbol{A} = \frac{1}{\mu_x}\left(\frac{\partial A_z}{\partial y} - \frac{\partial A_y}{\partial z}\right)\boldsymbol{i} + \frac{1}{\mu_y}\left(\frac{\partial A_x}{\partial z} - \frac{\partial A_z}{\partial x}\right)\boldsymbol{j} + \frac{1}{\mu_z}\left(\frac{\partial A_y}{\partial x} - \frac{\partial A_x}{\partial y}\right)\boldsymbol{k} \tag{2.48}$$

With the result of (2.47) and (2.48),

$$\begin{aligned} R_{11} &= -\int_{\Omega} \nabla N_i \times \frac{1}{\mu} \nabla \times \boldsymbol{A} \mathrm{d}v \\ &= -\left[\int_{\Omega} \left(\frac{1}{\mu_z}\frac{\partial N_i}{\partial y}\left(\frac{\partial A_y}{\partial x} - \frac{\partial A_x}{\partial y}\right) - \frac{1}{\mu_y}\frac{\partial N_i}{\partial z}\left(\frac{\partial A_x}{\partial z} - \frac{\partial A_z}{\partial x}\right)\right)\mathrm{d}v\right]\boldsymbol{i} \\ &\quad -\left[\int_{\Omega} \left(\frac{1}{\mu_x}\frac{\partial N_i}{\partial z}\left(\frac{\partial A_z}{\partial y} - \frac{\partial A_y}{\partial z}\right) - \frac{1}{\mu_z}\frac{\partial N_i}{\partial x}\left(\frac{\partial A_y}{\partial x} - \frac{\partial A_x}{\partial y}\right)\right)\mathrm{d}v\right]\boldsymbol{j} \\ &\quad -\left[\int_{\Omega} \left(\frac{1}{\mu_y}\frac{\partial N_i}{\partial x}\left(\frac{\partial A_x}{\partial z} - \frac{\partial A_z}{\partial x}\right) - \frac{1}{\mu_x}\frac{\partial N_i}{\partial y}\left(\frac{\partial A_z}{\partial y} - \frac{\partial A_y}{\partial z}\right)\right)\mathrm{d}v\right]\boldsymbol{k} \end{aligned} \tag{2.49}$$

For (2.40), the vector formulation is

$$\nabla(cd) = d\nabla c + c\nabla d$$

which leads to

$$\nabla\left(N_i \frac{1}{\mu_c}\nabla \cdot \boldsymbol{A}\right) = \nabla N_i \frac{1}{\mu_c}\nabla \cdot \boldsymbol{A} + N_i \nabla\left(\frac{1}{\mu_c}\nabla \cdot \boldsymbol{A}\right) \tag{2.50}$$

(2.50) is sorted out to:

$$N_i \nabla\left(\frac{1}{\mu_c}\nabla \cdot \boldsymbol{A}\right) = \nabla\left(N_i \frac{1}{\mu_c}\nabla \cdot \boldsymbol{A}\right) - \nabla N_i \frac{1}{\mu_c}\nabla \cdot \boldsymbol{A} \tag{2.51}$$

Substituting (2.51) into (2.40):

$$R_{12} = -\int_{\Omega} \nabla\left(N_i \frac{1}{\mu_c}\nabla \cdot \boldsymbol{A}\right) \mathrm{d}v + \int_{\Omega} \nabla N_i \frac{1}{\mu_c}\nabla \cdot \boldsymbol{A}\, \mathrm{d}v \tag{2.52}$$

The vector formulation is

$$\int_{\Omega} \nabla c\, \mathrm{d}v = \oint_{s} c\boldsymbol{n}\, \mathrm{d}s$$

The following form can be derived from (2.40):

$$R_{12} = -\oint_{s} N_i \left(\frac{1}{\mu_c}\nabla \cdot \boldsymbol{A}\right)\boldsymbol{n}\, \mathrm{d}s + \int_{\Omega} \nabla N_i \cdot \frac{1}{\mu_c}\nabla \cdot \boldsymbol{A}\, \mathrm{d}v \tag{2.53}$$

The continuity at the interface ($\frac{1}{\mu}\nabla \cdot \boldsymbol{A}$) becomes a natural interface condition. The surface integral of (2.53) will be canceled with the surface integral of (2.34), so only the volume integral term of

$$R_{12} = \int_{\Omega} \nabla N_i \frac{1}{\mu_c}\nabla \cdot \boldsymbol{A}\, \mathrm{d}v \tag{2.54}$$

The vector formulation is

$$\frac{1}{\mu_c}\nabla \cdot \boldsymbol{A} = \frac{1}{\mu_c}\left(\frac{\partial A_x}{\partial x} + \frac{\partial A_y}{\partial y} + \frac{\partial A_z}{\partial z}\right) \tag{2.55}$$

$$\nabla N_i = \frac{\partial N_i}{\partial x}\boldsymbol{i} + \frac{\partial N_i}{\partial y}\boldsymbol{j} + \frac{\partial N_i}{\partial z}\boldsymbol{k} \tag{2.56}$$

Substituting (2.55) and (2.56) into (2.54):

$$\begin{aligned} R_{12} &= \int_{\Omega} \nabla N_i \frac{1}{\mu_c} \nabla \cdot \boldsymbol{A} \, \mathrm{d}v \\ &= \int_{\Omega} \frac{1}{\mu_c} \frac{\partial N_i}{\partial x} \left(\frac{\partial A_x}{\partial x} + \frac{\partial A_y}{\partial y} + \frac{\partial A_z}{\partial z} \right) \mathrm{d}v \boldsymbol{i} \\ &\quad + \int_{\Omega} \frac{1}{\mu_c} \frac{\partial N_i}{\partial y} \left(\frac{\partial A_x}{\partial x} + \frac{\partial A_y}{\partial y} + \frac{\partial A_z}{\partial z} \right) \mathrm{d}v \boldsymbol{j} \\ &\quad + \int_{\Omega} \frac{1}{\mu_c} \frac{\partial N_i}{\partial z} \left(\frac{\partial A_x}{\partial x} + \frac{\partial A_y}{\partial y} + \frac{\partial A_z}{\partial z} \right) \mathrm{d}v \boldsymbol{k} \end{aligned} \tag{2.57}$$

For (2.41), we get

$$\begin{aligned} R_{13} &= \int_{\Omega} \sigma N_i \left(\frac{\partial A_x}{\partial t} + \frac{\partial}{\partial x} \left(\frac{\partial V}{\partial t} \right) \right) \mathrm{d}v \boldsymbol{i} \\ &\quad + \int_{\Omega} \sigma N_i \left(\frac{\partial A_y}{\partial t} + \frac{\partial}{\partial y} \left(\frac{\partial V}{\partial t} \right) \right) \mathrm{d}v \boldsymbol{j} \\ &\quad + \int_{\Omega} \sigma N_i \left(\frac{\partial A_z}{\partial t} + \frac{\partial}{\partial z} \left(\frac{\partial V}{\partial t} \right) \right) \mathrm{d}v \boldsymbol{k} \end{aligned} \tag{2.58}$$

Three components of the Galerkin residual of (2.32) can be obtained by synthesizing (2.49), (2.57) and (2.58):

$$\begin{aligned} R_x &= -\int_{\Omega} \left(\frac{1}{\mu_z} \frac{\partial N_i}{\partial y} \left(\frac{\partial A_y}{\partial x} - \frac{\partial A_x}{\partial y} \right) - \frac{1}{\mu_y} \frac{\partial N_i}{\partial z} \left(\frac{\partial A_x}{\partial z} - \frac{\partial A_z}{\partial x} \right) \right) \mathrm{d}v \\ &\quad + \int_{\Omega} \frac{1}{\mu_c} \frac{\partial N_i}{\partial x} \left(\frac{\partial A_x}{\partial x} + \frac{\partial A_y}{\partial y} + \frac{\partial A_z}{\partial z} \right) \mathrm{d}v \\ &\quad + \int_{\Omega} \sigma N_i \left(\frac{\partial A_x}{\partial t} + \frac{\partial}{\partial x} \left(\frac{\partial V}{\partial t} \right) \right) \mathrm{d}v \end{aligned} \tag{2.59}$$

$$\begin{aligned} R_y = &- \int_{\Omega} \left(\frac{1}{\mu_x} \frac{\partial N_i}{\partial z} \left(\frac{\partial A_z}{\partial y} - \frac{\partial A_y}{\partial z} \right) - \frac{1}{\mu_z} \frac{\partial N_i}{\partial x} \left(\frac{\partial A_y}{\partial x} - \frac{\partial A_x}{\partial y} \right) \right) \mathrm{d}v \\ &+ \int_{\Omega} \frac{1}{\mu_c} \frac{\partial N_i}{\partial y} \left(\frac{\partial A_x}{\partial x} + \frac{\partial A_y}{\partial y} + \frac{\partial A_z}{\partial z} \right) \mathrm{d}v \\ &+ \int_{\Omega} \sigma N_i \left(\frac{\partial A_y}{\partial t} + \frac{\partial}{\partial y} \left(\frac{\partial V}{\partial t} \right) \right) \mathrm{d}v \end{aligned} \tag{2.60}$$

$$\begin{aligned} R_z = &- \int_{\Omega} \left(\frac{1}{\mu_y} \frac{\partial N_i}{\partial x} \left(\frac{\partial A_x}{\partial z} - \frac{\partial A_z}{\partial x} \right) - \frac{1}{\mu_x} \frac{\partial N_i}{\partial y} \left(\frac{\partial A_z}{\partial y} - \frac{\partial A_y}{\partial z} \right) \right) \mathrm{d}v \\ &+ \int_{\Omega} \frac{1}{\mu_c} \frac{\partial N_i}{\partial z} \left(\frac{\partial A_x}{\partial x} + \frac{\partial A_y}{\partial y} + \frac{\partial A_z}{\partial z} \right) \mathrm{d}v \\ &+ \int_{\Omega} \sigma N_i \left(\frac{\partial A_z}{\partial t} + \frac{\partial}{\partial z} \left(\frac{\partial V}{\partial t} \right) \right) \mathrm{d}v \end{aligned} \tag{2.61}$$

To deduce R_0, the vector formulation is

$$\begin{aligned} \nabla \cdot \left(N_i \sigma \left(-\frac{\partial \boldsymbol{A}}{\partial t} - \nabla \left(\frac{\partial V}{\partial t} \right) \right) \right) = &\nabla N_i \cdot \sigma \left(-\frac{\partial \boldsymbol{A}}{\partial t} - \nabla \left(\frac{\partial V}{\partial t} \right) \right) \\ &+ N_i \nabla \cdot \left(\sigma \left(-\frac{\partial \boldsymbol{A}}{\partial t} - \nabla \left(\frac{\partial V}{\partial t} \right) \right) \right) \end{aligned} \tag{2.62}$$

(2.62) is sorted out to:

$$\begin{aligned} N_i \nabla \cdot \left(\sigma \left(-\frac{\partial \boldsymbol{A}}{\partial t} - \nabla \left(\frac{\partial V}{\partial t} \right) \right) \right) = &\nabla \cdot \left(N_i \sigma \left(-\frac{\partial \boldsymbol{A}}{\partial t} - \nabla \left(\frac{\partial V}{\partial t} \right) \right) \right) \\ &- \nabla N_i \cdot \sigma \left(-\frac{\partial \boldsymbol{A}}{\partial t} - \nabla \left(\frac{\partial V}{\partial t} \right) \right) \end{aligned} \tag{2.63}$$

Substituting (2.63) into (2.38)

$$\begin{aligned} R_0 &= \int_{\Omega} \nabla \cdot \left(N_i \sigma \left(-\frac{\partial \boldsymbol{A}}{\partial t} - \nabla \left(\frac{\partial V}{\partial t} \right) \right) \right) \mathrm{d}v - \int_{\Omega} \nabla N_i \cdot \sigma \left(-\frac{\partial \boldsymbol{A}}{\partial t} - \nabla \left(\frac{\partial V}{\partial t} \right) \right) \mathrm{d}v \\ &= \oint_{s} N_i \sigma \left(-\frac{\partial \boldsymbol{A}}{\partial t} - \nabla \left(\frac{\partial V}{\partial t} \right) \right) \cdot \boldsymbol{n} \mathrm{d}s - \int_{\Omega} \nabla N_i \cdot \sigma \left(-\frac{\partial \boldsymbol{A}}{\partial t} - \nabla \left(\frac{\partial V}{\partial t} \right) \right) \mathrm{d}v \end{aligned} \tag{2.64}$$

According to the conductor surface condition of $J_n = 0$, the surface integral term of (2.64) is zero, i.e.,

$$R_0 = -\int_{\Omega} \nabla N_i \cdot \sigma\left(-\frac{\partial \boldsymbol{A}}{\partial t} - \nabla\left(\frac{\partial V}{\partial t}\right)\right) \mathrm{d}v \tag{2.65}$$

Upon a simple vector operation, (2.65) can be rewritten as

$$\begin{aligned} R_0 = &\int_{\Omega} \sigma\left(\frac{\partial N_i}{\partial x}\left(\frac{\partial A_x}{\partial t} + \frac{\partial}{\partial x}\left(\frac{\partial V}{\partial t}\right)\right)\right) \mathrm{d}v + \int_{\Omega} \sigma\left(\frac{\partial N_i}{\partial y}\left(\frac{\partial A_y}{\partial t} + \frac{\partial}{\partial y}\left(\frac{\partial V}{\partial t}\right)\right)\right) \mathrm{d}v \\ &+ \int_{\Omega} \sigma\left(\frac{\partial N_i}{\partial z}\left(\frac{\partial A_z}{\partial t} + \frac{\partial}{\partial z}\left(\frac{\partial V}{\partial t}\right)\right)\right) \mathrm{d}v \end{aligned} \tag{2.66}$$

Non-Eddy Current Region

In non-eddy current region ω, conductivity $\sigma = 0$; the third term in (2.59), (2.60) and (2.61) will disappear, and $\mu = \mu_0$, based on the above deduction, the corresponding Galerkin residuals of (2.34) are as

$$\begin{aligned} R'_x = &-\int_{\omega} \left(\frac{1}{\mu_0}\frac{\partial N_i}{\partial y}\left(\frac{\partial A_y}{\partial x} - \frac{\partial A_x}{\partial y}\right) - \frac{1}{\mu_0}\frac{\partial N_i}{\partial z}\left(\frac{\partial A_x}{\partial z} - \frac{\partial A_z}{\partial x}\right)\right) \mathrm{d}v \\ &+ \int_{\omega} \frac{1}{\mu_0}\frac{\partial N_i}{\partial x}\left(\frac{\partial A_x}{\partial x} + \frac{\partial A_y}{\partial y} + \frac{\partial A_z}{\partial z}\right) \mathrm{d}v \end{aligned} \tag{2.67}$$

$$\begin{aligned} R'_y = &-\int_{\omega} \left(\frac{1}{\mu_0}\frac{\partial N_i}{\partial z}\left(\frac{\partial A_z}{\partial y} - \frac{\partial A_y}{\partial z}\right) - \frac{1}{\mu_0}\frac{\partial N_i}{\partial x}\left(\frac{\partial A_y}{\partial x} - \frac{\partial A_x}{\partial y}\right)\right) \mathrm{d}v \\ &+ \int_{\omega} \frac{1}{\mu_0}\frac{\partial N_i}{\partial y}\left(\frac{\partial A_x}{\partial x} + \frac{\partial A_y}{\partial y} + \frac{\partial A_z}{\partial z}\right) \mathrm{d}v \end{aligned} \tag{2.68}$$

$$\begin{aligned} R'_z = &-\int_{\omega} \left(\frac{1}{\mu_0}\frac{\partial N_i}{\partial x}\left(\frac{\partial A_x}{\partial z} - \frac{\partial A_z}{\partial x}\right) - \frac{1}{\mu_0}\frac{\partial N_i}{\partial y}\left(\frac{\partial A_z}{\partial y} - \frac{\partial A_y}{\partial z}\right)\right) \mathrm{d}v \\ &+ \int_{\omega} \frac{1}{\mu_0}\frac{\partial N_i}{\partial z}\left(\frac{\partial A_x}{\partial x} + \frac{\partial A_y}{\partial y} + \frac{\partial A_z}{\partial z}\right) \mathrm{d}v \end{aligned} \tag{2.69}$$

On the treatment of complicated material properties in the formulation and numerical implementation based on the potential sets, and the measurement and prediction of the corresponding material properties, can be found in the related chapters of this book or other related literatures.

References

1. J. C. Maxwell, "A treatise on electricity and magnetism," Vols. I and II, Clarendon Press, England, 1904.
2. J. A. Stratton. *Electromagnetic Theory*. McGraw-Hill Book Company, Inc., New York & London, 1941.
3. R. W. Clough, "The finite element method in plane stress analysis," Proc. of 2nd ASCE Conf. Electronic Computation, Pittsburgh, PA., pp. 345–378, 1960.
4. Fraeijs B.X.de Veubeke, "Displacement and equilibrium models in the finite element method, Stress Analysis (ed. by O. C. Zienkiewicz & G. Holister), New York: Wiley. 1965.
5. O. C. Zienkiewicz. *The finite element method*. Fourth edition. McGraw-Hill. 1994.
6. A. M. Winslow, "Numerical solution of the quasi-linear Poisson equation in a non-uniform triangle mesh," Journal of Computational Physics, vol. 2, 1967, pp. 149–172.
7. P. P. Silvester, "Finite element solution of homogeneous waveguide problems," Alta Frequenza, 38, 1969, pp. 313–317.
8. J. C. Nedelec, "Mixed finite elements in R^3", Numerische Mathematik, vol. 35, pp. 315–341, 1980.
9. C. J. Carpenter, "Comparison of alternative formulations of 3-dimensional magnetic-field and eddy-current problems at power frequencies," Proc.IEE, Vol. 124, No. 11 Nov., 1977, pp. 1026–1034.
10. C. W. Trowbridge, "Electromagnetic computing: the way ahead!" *IEEE Trans. on Magn.*, vol. 24, 1988, pp. 3159–3161.
11. A. Bossavit. *Computational electromagnetism (Variational formulations, complementarity, edge elements)*. Academic Press. 1998.
12. C. Feng (editor), *Electromagnetic Field* (2nd Edition, in Chinese). Higher Education Press, 1983.
13. J. Sheng, et al., *Numerical Analysis for Electromagnetic Fields (in Chinese)*. Science Press, 1984.
14. X. Wang, *Theory and Application of Electromagnetic Fields* (in Chinese). Science Press, 1986.
15. K. Zhou, *On Engineering Electromagnetic Field (in Chinese)*. Huazhong Engineering College Press, 1986.
16. Y. Tang. *Electromagnetic Field in Motor* (in Chinese). Science Press, 1982.
17. N. Takahashi, *Three Dimensional Finite Element Methods*. IEEJ, Japan, 2006.
18. P. Chen, L. Yan, and R. Yao, *Theory and Calculation of Motor Electromagnetic Field* (in Chinese). Science Press, 1986.
19. X. Ma, J. Zhang, and P. Wang, *Fundamentals of Electromagnetic Fields* (in Chinese). Tsinghua University Press, 1995.
20. M. Fan, and W. Yan, *Electromagnetic Field Integral Equation* (in Chinese). China Machine Press, 1988.
21. G. Ni (editor), *Principle of Engineering Electromagnetic Field*(in Chinese). Higher Education Press, 2002.
22. W. Yan, Q. Yang, and Y. Wang, *Numerical Analysis of Electromagnetic Fields in Electrical Engineering* (in Chinese). China Machine Press, Aug. 2005.

23. D. Xie, et al., *Finite Element Analysis of 3D Eddy Current Field*. China Machine Press (2nd Edition, in Chinese), Mar. 2008.
24. O. Biro and K. Preis, "Finite element analysis of 3-D eddy currents," *IEEE Trans. on Magn.*, vol. 26, 1990, pp. 418–423.
25. O. Biro, K. Preis, W. Renhart, K. R. Richter, and G. Vrisk, "Performance of different vector potential formulations in solving multiply connected 3-D eddy current problems," *IEEE Trans. on Magn.*, vol. 26, 1990, pp. 438–411.
26. N. Ida and J. P. A. Bastos. *Electromagnetics and calculation of fields* (second edition). Springer, 1997.
27. O. Biro, "Edge element in eddy current computations," Lecture of seminar on advanced computational electromagnetics, May 26, 1999.
28. G. Mur, Edge elements, their advantages and their disadvantages, *IEEE Trans. on Magn*., vol. 30, No. 5, 1994, pp. 3552–3557.
29. A. Kameari, "Three dimensional eddy current calculation using edge elements for magnetic vector potential," Applied electromagnetics in materials, 225(1989), Pergamon Press.
30. K. Fujiwara, "3D magnetic field computation using edge elements," Proc. of the 5th IGTE symposium on numerical field computation in electrical engineering, Graz, Austria, September 18–22, 1992, pp. 185–212.
31. A. Ahagon and K. Fujiwara, "Some important properties of edge shape functions," *IEEE Trans. on Magn.,* vol. 34, no. 5, Sep.1998, pp. 3311–3314.
32. M. Gyimesi and D. Ostergaard, "Non-conforming hexahedral edge elements for magnetic analysis," *IEEE Trans. on Magn*., vol. 34, no. 5, 1998, pp. 2481–2484.
33. J. S. van Welij, "Calculation of eddy currents in terms of H on hexahedra," *IEEE Trans. on Magn.*, vol. 21, no. 6, 1985, pp. 2239–2241.
34. A. Kameari, "Calculation of transient 3D eddy current using edge elements," *IEEE Trans. on Magn.*, vol. 26, no. 2, 1990, pp. 466–469.
35. Z. J. Cendes, "Vector finite elements for electromagnetic field computation," *IEEE Trans. on Magn.,* vol. 27, 1990, pp. 3958–3966.
36. A. Bossavit, "Solving Maxwell equations in a closed cavity and the question of 'spurious modes'," *IEEE Trans. on Magn.*, vol. 26, 1990, pp. 702–705.
37. Z. Ren, C. Li and A. Razek, "Hybrid FEM-BIM formulation using electric and magnetic variables," *IEEE Trans. on Magn*., vol. 28,1992, pp. 1647–1650.
38. A. Kameari and K. Koganezawa, "Convergence of ICCG method in FEM using edge elements without gauge condition," *IEEE Trans. on Magn.*, vol. 33, No. 2, March 1997, pp. 1223–1226.
39. G. Mur, "The finite element modeling of three-dimensional electromagnetic fields using edge and nodal elements," *IEEE Trans. on Antennas & Propagation*, vol. 41, No. 7, 1993, pp. 948–953.
40. K. Sakiyama, H. Kotera, and A. Ahagon, "3D electromagnetic field mode analysis using finite element method by edge element," *IEEE Trans. on Magn.*, vol. 26, no. 2, pp. 1759–1761, 1990.
41. M. L. Barton and Z. Cendes, "New vector finite elements for three-dimensional magnetic field computation," Journal of Applied Physics, vol. 61, No. 8, 1987, P. 3919–3921.
42. J. Wang and N. Ida, "Curvilinear and higher order 'edge' finite elements in electromagnetic field computation," *IEEE Trans. on Magn.*, vol. 29, No. 2, 1993, pp. 1491–1494.
43. K. Fujiwara, T. Nakata, and H. Ohashi, "Improvement of convergence characteristics of ICCG method for **A**-ϕ method using edge elements," *IEEE Trans. on Magn.*, vol. 32, no. 5, 1996, pp. 804–807.
44. O. Biro, K. Preis and K. R. Richter, "On the use of magnetic vector potential in nodal and edge finite element analysis of 3D magnetostatic problem," *IEEE Trans. on Magn*., vol. 32, no. 5, 1996, pp. 651–654.
45. J. B. Manges and Z. J. Cendes, "A generalized tree-cotree gauge for magnetic field computation," *IEEE Trans on Magn.,* Vol. 31, no. 3, 1995, pp. 1342–1347.

46. J. P. Webb, "Edge elements and what they can do for you?" *IEEE Trans. on Magn.*, vol. 29, No. 2, 1993, pp. 1460–1465.
47. C. Bedrosian, M. V. K. Chari, and J. Joseph, "Comparison of full and reduced potential formulations for low-frequency applications," *IEEE Trans. on Magn.*, vol. 29, no. 2, 1995, pp. 1321–1324.
48. P. Dular, "Local and global constraints in finite element modeling and the benefits of nodal and edge elements coupling," *ICS Newsletter*, Vol. 7, no. 2, 2000, pp. 4–7.
49. T. Nakata, N. Takahashi, K. Fujiwara, and T. Imai, "Investigation of effectiveness of edge elements," *IEEE Trans. on Magn.,* vol. 28, no. 2, 1992, pp. 1619–1622.
50. T. Nakata, N. Takahashi, K. Fujiwara, and P. Olszewski, "Verification of software for 3-D eddy current analysis using IEEJ model," Advances in electrical engineering software, 349 (1990), Springer-Verlag.
51. H. Yu, K. Shao, L. Li, and C. Gu, "Edge-nodal coupled method for computing 3D eddy current problems," *IEEE Trans. on Magn.*, vol. 33, no. 2,1997, pp. 1378–1381.
52. J. Lu, L. Li, and K. Shao, *Calculation of Three-dimensional Transient Eddy Current by Using Finite Edge Element*, Proceedings of the CSEE, vol. 13, no. 5, 1993:34–41.
53. J. Lu, K. Shao, L. Li, and K. Zhou, "A new method to solve 3D eddy current using edge element in terms of A in the whole region, Proc. of ICEF, 1992, "Electromagnetic Field Problems and Application," (ed. by Jian Baiton), pp. 294–297.
54. Z. Cheng, S. Gao, and L. Li, "Eddy Current Loss Analysis and Validation in Electrical Engineering," (supported by National Natural Science Foundation of China), ISBN 7-04-009888-1, Higher Education Press, 2001.